DESIGN CRITERIA FOR ELLIPTICAL CAVITIES

C. Pagani, D. Barni, A. Bosotti, P. Pierini,
INFN Milano, LASA, Via Fratelli Cervi 201, I-20090 Segrate (MI), Italy
G. Ciovati
TJNAF, 12000 Jefferson Av., Newport News, Virginia, USA

Abstract

In the framework of the TRASCO project, we have developed a set of criteria to guide the design of elliptical multicell SC cavities, supporting them with a few design tools to aid the geometry optimisation. In this paper we briefly summarize this work and the related codes we have implemented. Some examples are also given of their applications to cavity design, discussing the experimental results obtained so far to validate our design method.

1 INTRODUCTION

The optimum design of an elliptical cavity for particle acceleration is the consequence of a series of compromises between different parameters, ranging from RF to mechanics, and takes into account specific fabrication constrains.

Because of the wide number of applications, some of them very specific, we limit our discussion to multicell elliptical cavities with a minimum beta equal to ~ 0.5. Elliptical structures with lower betas are inefficient, because of filling and transit time factors, while single cells are usually required for low impedance rings where the design is dominated by the need of a very strong damping of the high order modes.

The guiding line of the work we performed in the last few years was to determine a general procedure to choose, for each application, the best compromise between electromagnetic and mechanical properties of one candidate cavity, having in mind the fabrication constrains, as derived from the experience of the TTF cavity production.

The first important result on this achievement has been to find an efficient parameterization for the cavity geometry that leaves a complete freedom in the cavity shape, while linking each aspect of the cavity performance to one, or maximum two, specific geometrical parameter.

Once we defined a suitable parameterization, we have implemented a procedure that allows tuning the cavity to the correct frequency without altering its main shape parameters. In order to do so, we wrote a tuning front-end [1] to drive automatically the use of Superfish [2], a well-established 2D RF analysis code. The front end assists also the design and tuning of end cells and the automatic generation and analysis (again with Superfish) of multi-cell structures, starting from the choice of the inner cell shape and of the external cells.

Furthermore, in order to make comparisons, all cavity geometries and results are stored in a cavity database.

Finally, our package has a post processor that allows mechanical calculations from the modeled cavity (including radiation pressures for Lorentz forces coefficient evaluation).

This new tool has been first applied to study in detail the RF cavities proposed in the context of the Collaboration between the Italian program TRASCO [3] and the French program ASH [4], both aiming at studies of a superconducting linac driver option for a nuclear waste transmutation system, possibly integrated in a multipurpose facility.

In defining the reference cavity geometries that are needed in order to start the construction and test of single cell and multi cell prototypes, both the electromagnetic and mechanical aspects have been taken fully into account.

As already said, the number of possible parameters involved in the design of a SC cavity is relatively big and, without a proper choice, it can be very hard to correlate a single geometrical parameter to the electromagnetic and mechanical performances of the cavity. In addition to that, the number of possible different strategies for the cell tuning to the correct frequency can complicate this correlation process, and a suitable tuning strategy helps to control more easily the cavity performances, including the mechanical aspects.

Note that the TRASCO and ASH programs aim mainly at continuous (CW) operation, and the design operating peak surface magnetic fields have been limited to 50 mT. While a stiffening structure for the lowest beta cavities is needed for vacuum load problems, no stringent requirements on the Lorentz force detuning have been set. The experience gained performing this cavity design, gave us the possibility of a further implementation of the design tools, which are now widely used and can be freely obtained [5].

In the following we describe the design procedure and discuss the design choices we put as a basis for the TRASCO-ASH [6] cavities and for those designed for SNS [7,8] and RIA [9]. As working example the SNS, β=0.61, cavity is used in this paper.

A comparison between most of the cavities designed so far will also be given, to show the many different possible optimization choices, which mainly depend on the project boundary conditions.

2 INFLUENCE OF CELL GEOMETRY

The parameterization described in reference 1 allowed us to finely control each aspect of the cavity performances in terms of one, or at most two, geometrical parameters. For sake of completeness, in Figure 1 the geometrical parameters chosen to describe the central cell of a bi-elliptical cavity are presented, while the correlation between performances and the seven parameters are summarized in the following list:

- The **cell length** (L) determines the cavity geometrical beta value.
- The cell **iris radius** (R_{iris}) is mainly determined by the cell-to-cell coupling requirements.
- The **side wall inclination** (α) **and position** (d) with respect to the iris plane can be set to achieve a tradeoff between electric and magnetic peak fields with a minor effect on cell-to-cell coupling.
- The **iris ellipse ratio** (r=b/a) is uniquely determined by the local optimization of the peak electric field.
- The **equator ellipse ratio** (R=B/A) is ruled by purely mechanical considerations and has no influence on the electromagnetic performances.
- The **cell radius** (D) is used for the frequency tuning without modifying any electromagnetic or mechanical cavity parameter.

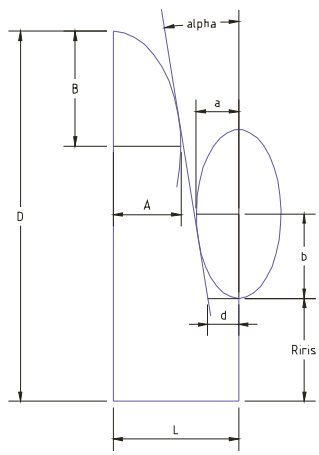

Figure 1: Cavity shape parametrization.

Each of the points listed above will be discussed in the following paragraphs, taking mainly the SNS β=0.61 cavity as a working example.

The tuning of the cell to the right frequency is then performed by varying the cell radius D without changing any of the other independent parameters (namely, R, r, d, α, R_{iris} and L). This is practically achieved by varying the equator ellipse parameter (A, B), but keeping their ratio (R) fixed. The distance between the ellipses centers, fulfilling the tangency condition, changes accordingly. In this manner the cavity shape, uniquely determined by the six independent parameters, is not affected by the tuning procedure.

We can now discuss the effect of the variation of each single geometrical parameter in the following paragraphs.

2.1 The equator aspect ratio R

The equator aspect ratio R=B/A is a free parameter for what concerns the electromagnetic π-mode design.

Figure 2 shows the electromagnetic parameters - Ep/Eacc (peak surface electric field over accelerating field, diamonds), Bp/Eacc (peak surface magnetic field over accelerating field, boxes), R/Q (triangles) and cell-to-cell coupling (stars) - as the R parameter is varied from a circle (R=1) to an ellipse with R=2. No changes can be seen from the plot, indicating that R can be chosen freely from the electromagnetic design.

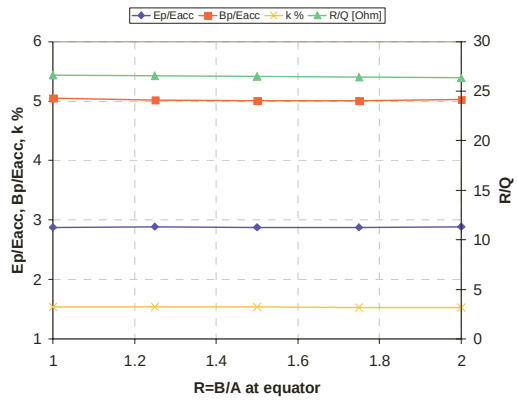

Figure 2: Electromagnetic parameters as a function of the equator aspect ratio, R.

This fact is due to our tuning strategy, in which the different geometries are Slater compensated at the equator region.

However, R has an impact on the mechanical performances of the cavity. Figure 3 shows the mechanical parameters – maximum stress in the structure (2 bar pressure, stars), tuning coefficient (frequency variations per unit elongation of the geometry, boxes) and two Lorentz coefficients (for a stiffening ring at 70 and 80 mm from the axis, diamonds) – as a function of R.

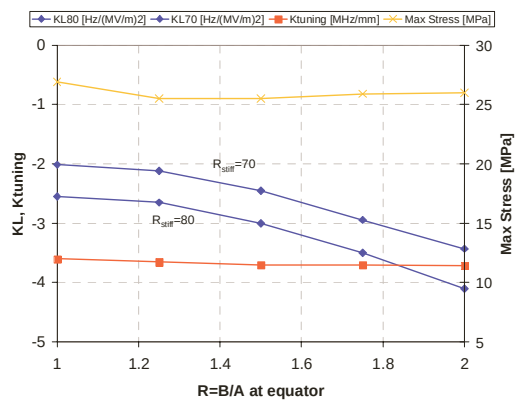

Figure 3: Mechanical parameters as a function of the equator aspect ratio, R.

2.2 The iris aspect ratio r

For any cavity geometry and parameters, there is an optimal value for the iris aspect ratio that minimizes the peak electric field with marginal influence on the other electromagnetic parameters.

Figure 4 shows the variation of the electromagnetic parameters (see description of Fig.2) as a function of the iris aspect ratio. A minimization of the peak electric field of about 10% can be achieved by choosing r=1.4.

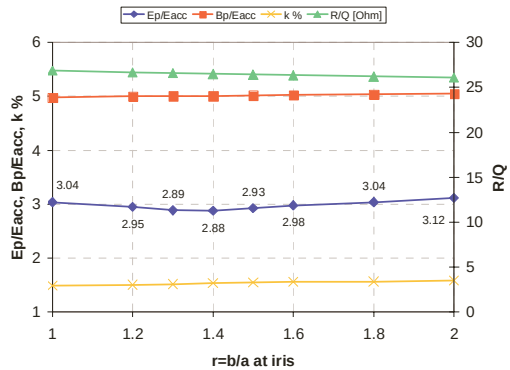

Figure 4: Electromagnetic parameters as a function of the iris aspect ratio, r.

The r parameter, conversely, has no influence on the mechanical performances of the cavity, as it can be shown by Figure 5.

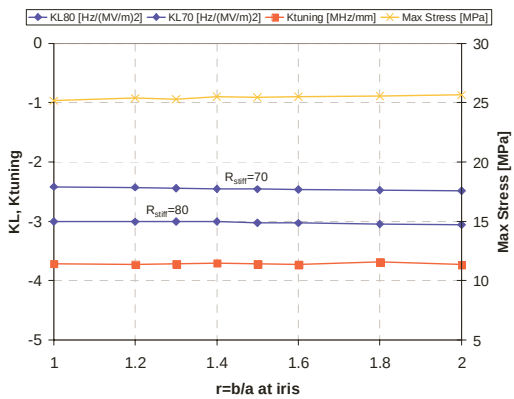

Figure 5: Mechanical parameters as a function of the iris aspect ratio, r.

2.3 The wall distance d

The wall distance parameter, d, is a useful knob to balance the electric and magnetic volumes for the cavity. Greater values of d mean greater distances of the wall from the iris, that is, a greater electric volume and, consequently a smaller magnetic volume at the equator, i.e. higher peak surface magnetic fields and lower peak surface electric fields.

However, the changes to the wall positions also have an influence on the cell-to-cell coupling parameter, if the iris radius is kept constant.

In Figure 6 we show the effect of the variation of d at a fixed Riris on the electromagnetic parameter. For each point the r has been chosen as the local minimum for the peak electric field. From the figure we can clearly see both the effect of balance between the peak fields (electric/magnetic), and the change in cell-to-cell coupling as the cell capacitive volume is varied.

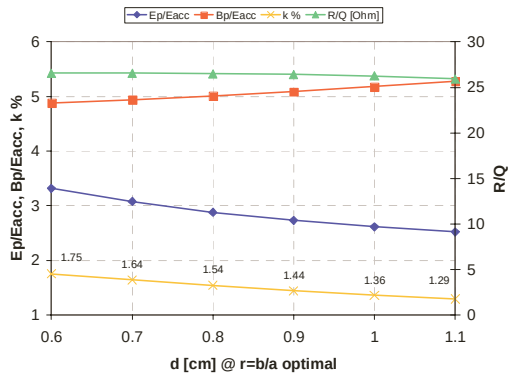

Figure 6: Electromagnetic parameters as a function of the wall distance, d, at fixed R_{iris}.

Figure 7 shows the effect of the wall distance d on the mechanical parameters. Smaller values of d achieve better mechanical performances both for the stress distribution and for the Lorentz forces coefficient.

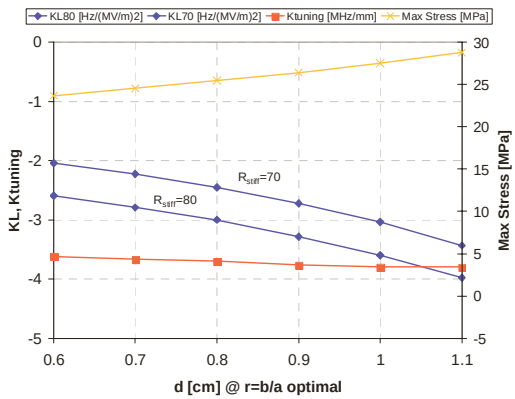

Figure 7: Mechanical parameters as a function of the wall distance, d, at fixed R_{iris}.

Since the cell-to-cell coupling is generally a design parameter, it can be useful to adjust the iris radius at each variation of the wall distance in order to keep this parameter constant.

Figure 8 and 9 show the electromagnetic and mechanical parameters as a function of the wall distance d, at the fixed cell-to-cell coupling value of 1.5 %.

Figure 8 shows also the R_{iris} parameter (stars) needed to obtain the fixed coupling value. The main effect of the variation of d is still a trade-off between peak electric and peak magnetic fields and, in addition to that, an R/Q decrease as the wall distance from the iris increases (due to the overall decrease of the cavity volume).

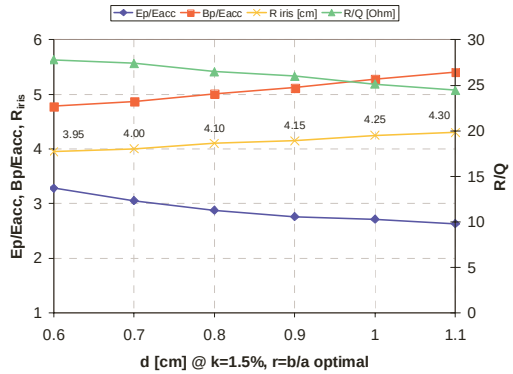

Figure 8: Electromagnetic parameters as a function of the wall distance, d, at fixed cell-to-cell coupling.

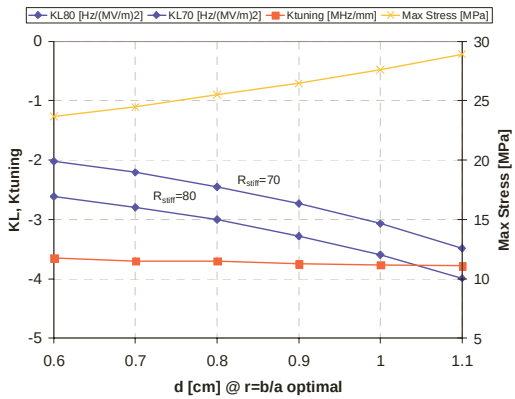

Figure 9: Mechanical parameters as a function of the wall distance, d, at fixed cell-to-cell coupling.

2.4 *The wall angle α*

Next, we proceed to examine the effect of variations of the wall inclination, the angle α. From Figure 10 we can see that the wall angle has a relatively small effect on the electromagnetic parameters: higher angles reduce the cavity magnetic volume (i.e. higher peak magnetic fields) and increase the electric volume (i.e. lower peak magnetic fields). However, Figure 11 shows that lower angle values are preferable for the Lorentz forces coefficient and the stress distribution.

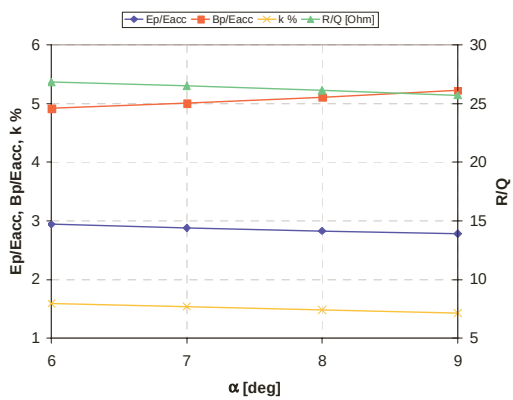

Figure 10: Electromagnetic parameters as a function of the wall inclination angle, α.

We should not, however, that the wall angle has also fabrication and cavity treatments constraints, since small values can be critical for the cavity chemistry and cleaning procedures.

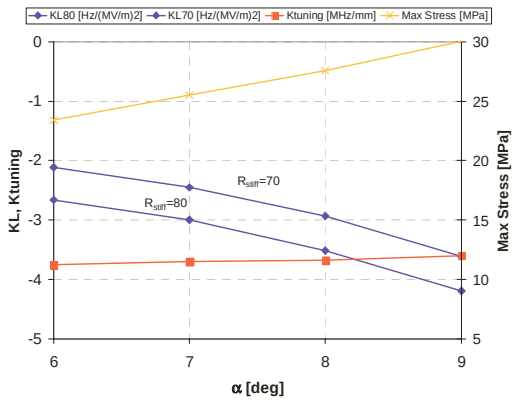

Figure 11: Mechanical parameters as a function of the wall inclination angle, α.

2.5 *The iris radius, R_{iris}*

The choice of the bore radius of the cavity at the iris needs to be performed taking into account the cell-to-cell coupling and the beam line aperture requirements. The possible necessity of a high coupling value for the main coupler can be accommodated by using a larger beam tube at the coupler side.

2.6 *Niobium thickness considerations*

The thickness of the niobium sheets highly affects the Lorentz forces detuning coefficient, even if, practically, its variation is limited because of material cost considerations, difficulties in shaping and considerations of the forces needed for cavity tuning.

Figure 12 shows the variation of the Lorentz forces coefficients for a niobium sheet thickness ranging from 3.3 to 4.3 mm (after a total typical material removal of 200 μm by the BCP procedure).

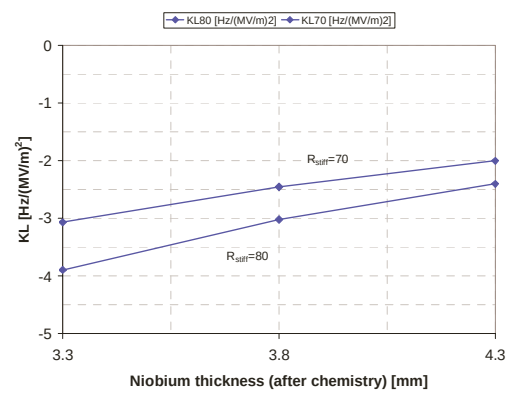

Figure 12: Lorentz forces detuning coefficients as a function of the niobium sheet thickness after a 200 μm chemistry removal. The original sheet thickness is then 200 μm higher.

2.7 The stiffening ring position and the tuning sensitivity

The position of the stiffening ring is extremely important for the mechanical stability of the cavity both under vacuum load and for the Lorentz force detuning. In Figure 13 we show the KL coefficient as a function of the stiffening ring position (distance from the beam axis). As a figure of merit for the evaluation of the Lorentz forces, we used in the previous paragraphs the coefficients computed for two reference stiffening radiuses: 70 and 80 mm from the beam axis. These are not necessarily the minimal values, as shown in Figure 13, but they are in a region where the KL is minimal and their final position could be left free within this range, for example, to tune the vibrational mode shifts. For these computations we used an initial niobium thickness of 4 mm (reduced by 200 μm of chemistry). The point at zero radius represent the behavior of the unstiffened cavity (with a fixed-length boundary condition for the calculation).

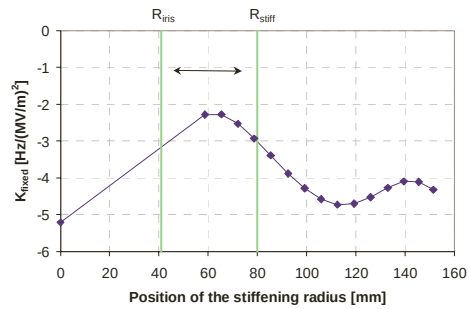

Figure 13: Variation of the Lorentz force detuning coefficient as a function of the stiffening ring position.

It is important to note that the stiffening ring should indeed reduce the cavity detuning under Lorentz forces (if the cavity is designed for pulsed operation), but should not jeopardize the cavity tunability or the possibility of achieving field flatness.

In Figure 14 we show the computed frequency displacement (squares, left scale) and the force needed (triangles, right scale) to shorten the cavity by 1 mm at the iris.

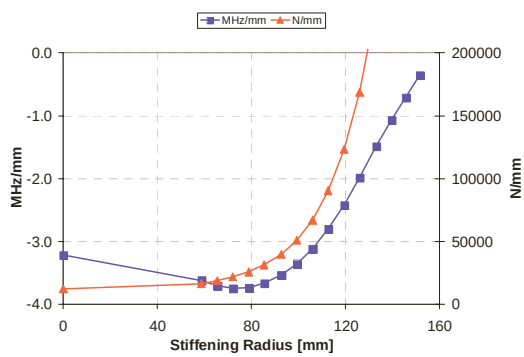

Figure 14: Frequency displacement and forces needed for a 1 mm cavity shortening vs ring position.

We can see that if the stiffening ring is displaced from the iris radius position, both the frequency displacement and the needed forces show a very steep increase, indicating indeed an increase of the cavity mechanical stiffness. So, although a local minimum for the Lorentz detuning coefficient exist with a high stiffening radius (see Figure 13), this choice, that could be preferred because of the reduced sensitivity to external boundary conditions (i.e. stiffness of the Tuner-Helium Tank system), it must be avoided because it complicates enormously the mechanical requirements for the cavity tuner, that need to deliver huge forces.

Furthermore, a stiffening ring too close to the equator may be harmful for the preservation of field flatness during the cavity tuning. Figure 15 shows the ratio between the needed tuning force and the obtained frequency displacement. Since the external cells do not have a stiffening ring (to be read in the picture at the stiffening radius equal to zero), the operation in a region where the curve is not flat will induce a non-homogeneous frequency displacement between the cells within the multi-cell structure, resulting in a loss of field flatness induced by the tuning.

In conclusion, the best position for the stiffening ring is that suggested by the first minimum of Fig.13, while the cavity longitudinal stiffness must be guaranteed by a very stiff Tuner-Helium Tank system.

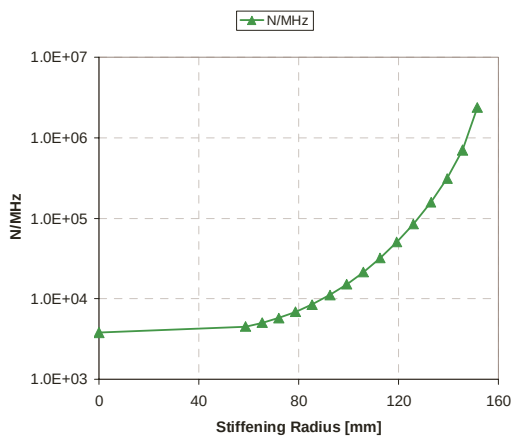

Figure 15: Net force per MHz frequency displacement, as a function of the stiffening ring position.

2.8 Endcells considerations

The endcells of a multicell cavity need different tuning algorithms. For the endcell at the small tube side we used the wall inclination parameter (α) for the frequency tuning, whereas for the endcell at the coupler side we implemented two different tuning strategies, either by varying α or by increasing the full end cell radius (thus requiring an additional die for fabrication). In fact, in order to compensate for the large coupler beam tube, magnetic volume has to be added to the end cell and this can be done very effectively by slightly increasing the cell

radius, without reducing too much (for mechanical considerations) the wall angle α. Another option, if the center cell has a large equator R, is to add volume by reducing R, limiting the necessary decrease of α (as in the TRASCO β=0.47 cavity).

For the TRASCO cavities, aiming at CW operation, the requirement on the Lorentz forces detuning is not stringent (as for SNS cavities) and so we preferred to design a 3-die cavity (one internal half-cell and two end cells) with an elliptical equator, whereas the SNS cavities are designed with four dies.

3 TRASCO AND SNS CAVITIES

Following these design criteria the cell shapes for the TRASCO [3,6] and SNS [7] cavities have been analyzed and characterized. The lowest beta cavity, β=0.47, that has been proposed but not included in the SNS design, has been re-proposed for the RIA design [9]. After the internal cell shapes the full multicell cavities have been designed. In all designs, but in the symmetrical RIA (see below), the beam tube at the cavities coupler side was increased, to improve the power coupling. Table 1 lists the cavity characteristics.

In the following we will give some justifications and comments on the design parameters of these cavity groups, explaining the differences and, where possible, the rationales of them. The SNS, and RIA, cavities could take advantage of a better understanding of the full parametrization we developed for the TRASCO cavities, the only minor limits being determined by the urgency of producing working prototypes, including a complete engineering of the ancillary components and the fabrication tools, leaving no time for a second order optimization.

3.1 The TRASCO/ASH cavity design

As stated above, the major criteria at the basis of the TRASCO/ASH cavity design have been the minimization of the ratio between the maximum magnetic field and the accelerating gradient, even if this choice slightly penalized the maximum value of the peak electric field for a given value of the cavity accelerating voltage. In particular, for the linac design, a peak magnetic field limit at 50 mT has been set.

Also, since our engineering effort were limited and the projects are still in an R&D phase (with no immediate commitments and boundary conditions depending on the construction of accelerator modules), also the mechanical construction was set simpler with respect to SNS and it is based on the three dies scheme, for the fabrication of each cavity beta family. Furthermore, one needs to remember that a linac CW operation was considered because of the foreseen ADS application, and hence the Lorentz force detuning coefficient did not play a role in the design of the stiffening system, with respect to the constraints on mechanical stability under vacuum.

Both the cell-to-cell coupling and the value for the Lorentz force detuning coefficient have been taken into account, but not considered as driving parameters. In particular, because of the promising results from our PIC code simulations [10], giving wide margins for the formation of dangerous beam halos, the cell-to-cell coupling has been limited, having in mind the scaling from TTF (which is 1.87% for a 9-cell cavity) and considering that the criticality of the mechanical tolerances increases as the cavity beta decreases. This justifies the different cell-to-cell coupling chosen for the first two cavity families, β=0.47 and β=0.65, respectively equal to 1.34% and 1.1%. In the case of the highest beta, β=0.85, a conservative value of 1.28% has been selected because it can be easily achieved without penalizing the peak magnetic field value.

3.2 The SNS cavity design

The cavity requirements for the SC SNS linac are dominated by the requirement of pulsed operation. Moreover the SNS design set a stringent limit of 27.5 MV/m of peak electric field (instead of magnetic) and a Lorentz forces coefficient of about -3 Hz/(MV/m)^2 (dominating the cost of the RF system). In this case a round equator was chosen, in order to minimize the KL factor and 4 die cavities have been designed, with a stiffening ring at a radius of 70-80 mm (the final position to be fixed after the first multicell prototypes at TJNAF) in order to finely control the longitudinal mechanical eigenfrequencies of the cavities. A different compromise between magnetic and electric volume has also been chosen, because of the limiting field criterion based on peak electric field.

A slightly better optimization of the cavity symmetry, with respect to the Lorentz force detuning would have been possible, given more time for optimization. Because of the dominant effect of the weakness of the external cavity system, composed by the helium tank and the tuner, the practical consequence of this further optimization looks negligible.

The 1.5% cell-to-cell coupling has been set as a compromised boundary condition. An equal value for the two betas is a good choice for HOM considerations.

3.3 The RIA cavity design

While in the SNS linac design the switch from the normal conducting linac to the superconducting linac has been set around 200 MeV, the RIA proposal envisages the use of superconducting cavities soon after the beam reaches 1.5 MeV/n. For this purpose a β=0.47 cavity has been designed [9], on the basis of most of the SNS design work, keeping in mind that the stringent constraints on the Lorentz force detuning should not be enforced for the CW operation of RIA. However, in this case a stiffening ring is still needed (as in the TRASCO 0.47 case) for the cavity stability under vacuum load.

Table 1: TRASCO-ASH, SNS and RIA cavity parameters

TRASCO-ASH CAVITIES									
Frequency [MHz]	704.4								
Cavity β – geometrical	**0.47**			**0.66**			**0.85**		
Cavity β – effective	0.5			0.68			0.87		
Number of dies	3			3			3		
Half-cell type	Int.	Ext left	Ext right	Int.	Ext. left	Ext. right	Int.	Ext. left	Ext. right
Half-cell length [mm]	50	50	50	70	70	70	90	90	90
Iris radius [mm]	40	40	65	45	45	65	50	50	65
Equator ellipse ratio, R	1.6	1.7	1	1	1.1	1	1	1.1	1
Iris ellipse ratio, r	1.3	1.3	1.3	1.3	1.3	1.3	1.4	1.4	1.4
Wall angle [deg]	5.5	5.98	4.84	8.5	8.85	5.6	8.5	9.1	5.74
Wall distance [mm]	7	7	6	10	10	10	10	10	8
Cell-to-cell coupling [%]	1.35			1.1			1.28		
Phys. cavity length [mm]	830			1050			1460		
Number of cells	5			5			6		
Cavity E_{peak}/E_{acc}	3.57			2.61			2.35		
Cavity B_{peak}/E_{acc} [mT/(MV/m)]	5.88			4.88			4.07		
Cavity R/Q [Ohm]	159			315			597		
Stiffening radius [mm]	70			Under discussion			N/A		
KL [Hz/(MV/m)^2] (inner)	-7			w/o –7.8/-2.7 @ 70 mm			-3.4		

SNS CAVITIES								
Frequency [MHz]	805							
Cavity β – geometrical	**0.61**				**0.81**			
Cavity β – effective	0.63				0.83			
Number of dies	4				4			
Half-cell type	Int.	Ext. left	Ext right 1	Ext right 2	Int.	Ext left	Ext. right 1	Ext. right 2
Half-cell length [mm]	56.8	56.8	56.8	56.8	75.5	75.5	75.5	75.5
Iris radius [mm]	43	43	43	65	48.8	48.8	48.8	70
Equator ellipse ratio, R	1	1	1	1	1	1	1	1
Iris ellipse ratio, r	1.7	1.5	1.7	1.5	1.8	1.6	1.8	1.6
Wall angle [deg]	7	8.36	7	10	7	10.07	7	10
Wall distance [mm]	11	10	11	10	15	13	15	13
Cell-to-cell coupling [%]	1.53				1.52			
Phys. cavity length [mm]	1000				1240			
Number of cells	6				6			
Cavity E_{peak}/E_{acc}	2.72				2.19			
Cavity B_{peak}/E_{acc} [mT/(MV/m)]	5.73				4.72			
Cavity R/Q [Ohm]	279				485			
Stiffening radius [mm]	70-80				70-80			
KL [Hz/(MV/m)^2] (inner)	-2.9/-3.4				-0.7/-0.8			

RIA CAVITIES						
Frequency [MHz]	805					
Cavity type	SNS like - asymmetrical				symmetrical	
Cavity β – geometrical	**0.47**				**0.47**	
Cavity β – effective	0.49				0.49	
Number of dies	4				2	
Half-cell type	Int.	Ext. left	Ext right 1	Ext right 2	Int.	Ext. left & right
Half-cell length [mm]	43.9	43.9	43.9	43.9	43.9	43.9
Iris radius [mm]	38.6	38.6	38.6	60	38.6	38.6
Equator ellipse ratio, R	1	1	1	1	1	1
Iris ellipse ratio, r	1.45	1.3	1.45	1.3	1.45	1.3
Wall angle [deg]	6.5	7.2	6.5	9	6.5	7.2
Wall distance [mm]	8.5	8	8.5	8	8.5	8
Cell-to-cell coupling [%]	1.5				1.5	
Phys. cavity length [mm]	820				760	
Number of cells	6				6	
Cavity E_{peak}/E_{acc}	3.41				3.34	
Cavity B_{peak}/E_{acc} [mT/(MV/m)]	6.92				6.61	
Cavity R/Q [Ohm]	160				173	
Stiffening radius [mm]	70-80				70-80	
KL [Hz/(MV/m)^2] (inner)	-5/-6				-5/-6	

4 MULTIPACTING AND HOMs

We want to conclude this paper noting that, in our design criteria for cavity design optimization, multipactoring and Higher Order Modes have not been included as design constraints. This choice has been originally dictated by the difficulty to find, among the different treatment of the two problems as given by different experts, a suitable and reliable cavity geometry parametrization that clearly indicates *a priori* criteria to avoid the occurrence of major problems. Conversely a wide experience on multicell elliptical cavities operating in different Labs suggested that these kind of cavities, when properly treated and handled, are not multipactoring limited and the higher order modes, excited by the beam, can be efficiently damped by properly designed HOM couplers.

In practice, we developed criteria to optimize the cavities only on the basis of electromagnetic and mechanical considerations, leaving the multipacting and HOM issues to *a posteriori* calculations. As we expected, these calculations have confirmed the validity of the designs.

Prototypes of most of the cavities discussed in this paper have been realized and successfully tested [11-13]. Expected multipactoring levels, when occurred, were easily processed. The design of HOM couplers seems not to present major problems.

REFERENCES

[1] P. Pierini et al., "Cavity Design Tools and Applications to the TRASCO Project", 9th Workshop on RF Superconductivity, Santa Fe , Nov. 1-5, 1999.
[2] J. Billen and L.M. Young, "POISSON SUPERFISH", LA-UR-96-1834.
[3] C. Pagani et al., "Status of the INFN High Current SC Proton Linac for Nuclear Waste Transmutation", Proceedings of the XIX Linac Conf. Chicago Aug. 23-28, 1998, p. 1013
[4] H. Safa, "Superconducting Proton Linac for Waste Transmutation", 9th Workshop on RF Superconductivity, Santa Fe , Nov. 1-5, 1999.
[5] The BuildCavity code can be freely obtained by requesting it to Paolo.Pierini@mi.infn.it.
[6] J.L. Biarrotte et al., "704 MHz Superconducting Cavities for a High Intensity Proton Accelerator", in 9th Workshop on RF Superconductivity, Santa Fe , Nov. 1-5, 1999.
[7] J. Alessi et al. "SNS Preliminary Design Report", SNS/ORNL Tech Note, November 1999.
[8] C. Pagani, "Cavity Design Criteria for SNS", SNS Cavity Shape Workshop, TJNAF, April 12-13, 2000.
[9] D. Barni et al., "A bg=0.472 Cavity for RIA – A proposal –" TJNAF Internal Note, Jlab-TN-01-014.
[10] P.Pierini, "A Multigrid Based Approach to Modelling a High Current Superconducting Linac for Waste Transmutation", Proceedings of the ICAP98, Monterey, Sept. 14-18, 1998.
[11] G. Ciovati et al., "Superconducting Prototype Cavities For The Spallation Neutron Source (SNS) Project", PAC2001, Chicago.
[12] C. C. Comptom et al.,"Niobium Cavity Development For the High-Energy Linac of the Rare Isotope Accelerator", PAC2001, Chicago.
[13] C. Pagani, "SRF Activities at INFN Milano – LASA", These Proceedings.